RECONFIGURABLE INTELLIGENT SURFACES-ENABLED EDGE COMPUTING: A LOCATION-AWARE TASK OFFLOADING FRAMEWORK

Md Sahabul Hossain[1], Nafis Irtija[1], Maria Diamanti[2], Fisayo Sangoleye[1], Eirini Eleni Tsiropoulou[1], Symeon Papavassiliou[2]
[1]Department of Electrical and Computer Engineering, University of New Mexico, Albuquerque, NM, USA, 87131 (email: mhossain1@unm.edu, nafis@unm.edu, fsangoleye@unm.edu, eirini@unm.edu), [2]School of Electrical and Computer Engineering, National Technical University of Athens, Athens, Greece, 15780 (email: mdiamanti@netmode.ntua.gr; papavass@mail.ntua.gr)

NOTE: Corresponding author: Symeon Papavassiliou, papavass@mail.ntua.gr

Abstract *– In this paper, an energy efficient task offloading mechanism in a Multiaccess Edge Computing (MEC) environment is introduced, based on the principles of contract theory. The technology of Reconfigurable Intelligent Surfaces (RISs) is adopted and serves as the enabler for energy efficient task offloading, from the perspective of location-awareness and improved communication environment. Initially a novel positioning, navigation, and timing solution is designed, based on the RIS technology and an artificial intelligent method that selects a set of RISs to perform the multilateration technique and determine the Internet of Things (IoT) nodes' positions in an efficient and accurate manner is introduced. Being aware of the nodes' positions, a maximization problem of the nodes' sum received signal strength at the MEC server where the nodes offload their computing tasks is formulated and solved, determining each RIS element's optimal phase shifts. Capitalizing on these enhancements, a contract-theoretic task offloading mechanism is devised enabling the MEC server to incentivize the IoT nodes to offload their tasks to it for further processing in an energy efficient manner, while accounting for the improved nodes' communications and computing characteristics. The performance evaluation of the proposed framework is obtained via modeling and simulation under different operation scenarios.*

Keywords – Edge computing, energy efficiency, positioning, navigation, and timing solution, reconfigurable intelligent surfaces, task offloading

1. INTRODUCTION

In the forthcoming 6G networks, the number of Internet of Things (IoT) devices and their generated data will experience a phenomenal growth, calling for a green communication solution and high-performance low-latency computing services. Towards supporting the computing needs of the next generation IoT devices, the Multiaccess Edge Computing (MEC) technology has emerged as a promising paradigm [1], providing computing resources at the edge of a wireless network by incorporating MEC servers at the next generation Node Bs (gNBs) [2]. The IoT devices can partially or fully offload their computing tasks to the edge servers in order to further process them, while considering their latency and energy constraints [3]. This way they manage to increase their computing capabilities and services they may support, by migrating computation to more resourceful devices, located nearby, such as edge nodes, fog nodes, base stations or access points. At the same time, the recent introduction of Reconfigurable Intelligent Surface (RIS) technology, provides the vehicle for realizing energy efficient communication in next generation wireless networks [4, 5]. The RISs are constructed based on engineered metamaterials and they appropriately reflect the multipath propagated signal via creating a constructive beam, thus, enabling the software-based control of the signals' electromagnetic properties [6]. Hence, by optimally controlling the phase shifts of the RIS elements, the overall received signal strength can be improved, resulting in superior energy efficiency [7, 8]. Last, but not least, in order to exploit the advantages of the aforementioned emerging technologies at their full potential, in supporting various applications with different communications and computing requirements, accurate and cost efficient positioning, navigation and timing services are required [9].

In this paper, we design a RIS-enabled location-aware task offloading mechanism in edge computing environments. In particular, we initially introduce a RIS-based positioning, navigation, and timing solution enabling the IoT devices to accurately determine their position in a real-time manner under scenarios of Global Positioning System (GPS) denial [10]. Based on the IoT devices' accurate positioning, we design a contract-theoretic task offloading mechanism to support the IoT devices' green computing. Throughout this process we determine the RIS elements' optimal phase shifts to realize the energy efficient communication and computing in the system.

1.1 Related work

Several recent research works have focused on the *communications field* studying the use of RISs to improve the system's energy efficient communication. In [11], the ground-to-air RIS-assisted links are optimized by

appropriately controlling the RIS elements' phase shifts in order to maximize the coverage and reliability of the considered Unmanned Aerial Vehicles (UAVs) communications system. Towards jointly optimizing the beamforming construction at the RIS elements, a fractional programming approach is introduced in [12]. The authors optimize the beamforming to maximize the uplink sum rate of all the users, and they examine the problem under perfect and imperfect channel state information. A similar approach is proposed in [13] focusing on maximizing the users' downlink sum rate while considering a multiple- input single-output communication system. Moreover, focusing on the downlink communication, a joint optimization of the transmit power allocation and the RIS el- ements' phase shifts to maximize the overall system's energy efficiency is introduced in [14].

The research on the RISs' benefits in terms of improving the system's energy efficiency has been extended by jointly examining the *computing and communication characteristics* of the system. The problem of minimizing the users' sum energy consumption is studied in [15] by jointly optimizing the users' transmission power and time, decoding order, amount of data offloaded to a single MEC server, and the RIS elements' phase shifts. Similarly, in [16, 17], the authors maximize the total amount of processed data by a MEC server, by further optimizing the received beamforming vectors by the MEC server and the users' energy partition among the local data processing on their devices and offloading data to the MEC server. Towards improving the overall MEC system's computing capability, the wireless powered technology is adopted in [18]. The authors introduce a scheduling mechanism by jointly optimizing the users' task offloading decisions, the RIS elements' phase shifts, and the users' energy harvesting time.

However, all the aforementioned approaches make the fundamental assumption that the IoT nodes, know their exact position while deciding their optimal task offloading strategy and their corresponding transmission power. This assumption is often quite unrealistic and optimistic, as the Global Navigation Satellite System (GNSS)-based Positioning, Navigation, and Timing (PNT) services suffer from limited availability in indoor environments [19], instability due to satellite signals interference, jamming, and spoofing [20]. Towards alleviating the burden of GPS denial, several ground-based PNT solutions have been introduced, such as the pseudolites and Locata systems [21], the distance measuring equipment networks [22], and the passive wide area multilateration technology [23]. The common characteristic of these PNT solutions is the utilization of at least four signals stemming from the ground base stations and the multilateration method to determine the target's (IoT nodes) position. The RIS technology has been recently used as a promising alternative to determine the gNBs' position, taking into account that the aforementioned ground-based solutions suffer from high infrastructure costs and limited coverage [24].

1.2 Contributions and outline

In this paper, a location-aware task offloading mechanism is introduced based on the principles of contract theory and utilizing the RIS technology. Initially, a novel PNT solution is proposed based on the RIS technology and an artificial intelligent method to select a set of RISs to perform the multilateration technique and determine the IoT nodes' positions in an accurate manner. Given the IoT nodes' positions, a maximization problem of the nodes' sum received signal strength at a MEC server, when the nodes offload their computing tasks to it, is formulated and solved via determining each RIS elements' optimal phase shifts, thus, introducing an energy efficient data transmission process. Towards further improving the system's energy efficiency, a contract-theoretic task offloading mechanism is introduced enabling the MEC server to incentivize the IoT nodes to offload their computing tasks to it for further processing in an energy efficient manner, while accounting for the nodes' communications and computing characteristics. The main contributions of this research work are summarized below.

1. A multi-IoT nodes single-MEC server integrated communications and computing environment enabled by multiple RISs is considered. A novel ground-based PNT solution is introduced to accurately determine the IoT nodes' position. Specifically, a reinforcement learning framework is proposed to enable each IoT node to select three RISs from the available ones in its environment for facilitating the realization of the PNT service, while the multilateration technique is adopted to determine the nodes' position in a distributed manner.
2. Each RIS's elements' phase shifts are optimized in order to maximize the nodes' sum received signal strength during the nodes task offloading process. This approach can result in decreasing the nodes' uplink transmission power, thus, improving the system's energy efficient operation.
3. A novel contract-theoretic task offloading mechanism is introduced accounting for the nodes' communications and computing characteristics. The latter ones define each node's type, which is of a continuous nature and the node's effort in terms of offloading its computing tasks to the MEC server in an energy efficient manner. The MEC server offers personalized rewards to the nodes in order to incentivize their energy efficient operation. The realistic scenario of incomplete information of the nodes' types from the MEC server's perspective is studied.

The remainder of this paper is organized as follows. Section 2 presents the system model and an overview

Table 1 – Summary of key notations

Notation	Description
$N = \{1, \dots, n, \dots, \lvert N \rvert\}$	Set of nodes
$\mathcal{R} = \{\mathcal{R}_1, \dots, \mathcal{R}_r, \dots, \mathcal{R}_{\lvert\mathcal{R}\rvert}\}$	Set of RISs
$\mathfrak{r}_n = (x_n, y_n, z_n)$	Node's coordinates
$d_{n,gNB}$ [m]	Node's distance from the MEC server
A_n	Node's computing task
B_n [bits]	Node's task's bits
ϕ_n [CPU Cycles/bits]	Node's task's computing intensity
C_n [CPU Cycles]	Node's task's number of CPU Cycles
P_n [Watts]	Node's uplink transmission power
Pr^{LoS}	probability of LoS communication
$\mathfrak{r}_{gNB} = (x_{gNB}, y_{gNB}, z_{gNB})$	gNB/MEC server's coordinates
$\alpha, \beta \in \mathbb{R}^+$	Positive constants depending on the communication environment
f_c [Hz]	Carrier frequency
θ [rad]	Elevation angle
$\mathcal{P}_{LoS}, \mathcal{P}_{NLoS}$	Path loss in the LoS and NLoS communication scenarios
η_{LoS}, η_{NLoS}[dB]	Excessive path loss exponents in the LoS and NLoS communication scenarios
c [m/s]	Speed of light
$\gamma \in \mathbb{R}^+$	Path loss exponent depending on the communication environment
$\mathcal{P}$	Overall expected path loss
$\mathcal{E} = \{1, \dots, e, \dots, \lvert\mathcal{E}\rvert\}$	Set of RIS's elements
$\omega_e \in [0, 2\pi)$	Element's phase shift
$\Omega_r = diag(e^{j\omega_1}, \dots, e^{j\omega_{\lvert\mathcal{E}\rvert}})$	RIS's diagonal reflection matrix
$g_{n,gNB}$	Channel gain of the direct communication link between the IoT node n and the gNB/MEC server
$\tilde{g}$	Random variable
$\mathbf{g}_{n,r}$	Channel gain of the link between the IoT node n and each RIS r
ζ	Path loss among the node n and the RIS $\mathcal{R}_r$ at the reference point of 1m
$d_{n,r}$	Distance among the node n and the RIS r
$\lambda[m]$	Carrier signal's wavelength
δ	Antenna separation
$\phi_{n,r}$	Cosine of the arrival angle of the node's n transmitted signal at the RIS r
$\mathbf{g}_{r,gNB}$	Channel gain of the link between each RIS $\mathcal{R}_r$ and the gNB/MEC server
κ	Rician factor
G_n	Total channel gain
R_n	Node's data rate
$W[Hz]$	System's bandwidth
I_0	Power of the Additive White Gaussian Noise

Table 2 – Summary of key notations (cont.)

Notation	Description
$\mathcal{S} = \{s_1, \dots, s_s, \dots, s_{\lvert\mathcal{S}\rvert}\}$	Set of possible RISs strategies
$GDOP(s_s)$	Node's Geometric Dilution of Precision
$f(s_s)$	Node's reward
P	Node's strategy selection probability
$\mu_1, \mu_2 \in [0, 1]$	Learning parameters
Δt	gNB's and the node's time clock offsets
$\mathcal{J}^{(ite')}, \mathcal{R}es^{(i')}$	Jacobian and Residual matrices
t_n	IoT node's type
$f(t)$	Probability density function of nodes' types
$q(t_n)$	IoT node's effort
$r(t_n)$	IoT node's reward
U_n	IoT node's utility function
$\mathfrak{c} \in \mathbb{R}^+$	IoT node's cost
$\mathfrak{e}(r(t_n))$	Evaluation function
U_{MEC}	MEC server's utility function
$\mathfrak{c} \in \mathbb{R}^+$	MEC server's cost

of the proposed framework. Section 3 introduces the RIS-enabled PNT solution, while Section 4 determines the RIS elements' optimal phase shifts to support the system's energy efficient operation. Section 5 designs and analyzes the proposed contract-theoretic task offloading mechanism, while Section 6 presents a detailed performance evaluation of the overall proposed framework. Finally, Section 7 concludes the paper.

2. SYSTEM MODEL AND FRAMEWORK OVERVIEW

2.1 RIS-enabled integrated communications and computing

We consider a multi-IoT nodes single-MEC server integrated communications and computing environment consisting of multiple RISs supporting both the PNT services and the energy efficient task offloading process. An overview of the considered environment is presented in Fig. 1. The set of nodes is denoted as $N = \{1, \dots, n, \dots, |N|\}$, and the set of RISs is $\mathcal{R} = \{\mathcal{R}_1, \dots, \mathcal{R}_r, \dots, \mathcal{R}_{|\mathcal{R}|}\}$. The MEC server is attached to the gNB. Each node has unknown coordinates $\mathfrak{r}_n = (x_n, y_n, z_n)$ and its corresponding distance from the MEC server is $d_{n,gNB}$ [m]. Also, each IoT node has a computing task $A_n = (B_n, C_n, \phi_n)$ that needs to process, where B_n [bits] denotes the total task's bits, ϕ_n [CPU Cycles/bits] represents the computing task's intensity, and $C_n = \phi_n \cdot B_n$ [CPU Cycles] is the number of CPU cycles in order for the computing task A_n to be executed. Each IoT node can fully offload its computing task to the MEC server for further processing in order to save its battery from locally executing its task. For the purposes of offloading, the node needs to wirelessly transmit its data with uplink transmission power P_n [Watts]. The key notation used in the paper is summarized in tables 1 and 2.

During the nodes' task offloading, the nodes can have both Line of Sight (LoS) communication with the MEC server and non-LoS (NLoS) communication due to the signals' reflections on the RISs. The probability of LoS communication is:

$$Pr^{LoS}(z_{gNB}, d_{n,gNB}) = \frac{1}{1 + \alpha e^{-\beta(\theta - \alpha)}}, \qquad (1)$$

where $\mathfrak{r}_{gNB} = (x_{gNB}, y_{gNB}, z_{gNB})$ are the gNB/MEC server's coordinates, $\alpha, \beta \in \mathbb{R}^+$ are positive constants depending on the communication environment, e.g., urban, rural, and the carrier frequency $f_c[Hz]$ and $\theta = \frac{180}{\pi} sin^{-1}(\frac{z_{gNB}}{d_{n,gNB}})[rad]$ denotes the elevation angle between the node and the gNB/MEC server. The corresponding path loss in the LoS (Eq. *(2)*) and NLoS (Eq. *(3)*) communication scenarios are derived as follows:

$$\mathcal{P}_{LoS}(d_{n,gNB}) = \eta_{LoS}(\frac{4\pi f_c d_{n,gNB}}{c})^{\gamma}, \qquad (2)$$

$$\mathcal{P}_{NLoS}(d_{n,gNB}) = \eta_{NLoS}(\frac{4\pi f_c d_{n,gNB}}{c})^{\gamma}, \qquad (3)$$

where $\eta_{LoS}, \eta_{NLoS}[dB]$ denote the excessive path loss exponents, with $\eta_{NLoS} > \eta_{LoS} > 1$, $c[m/s]$ is the speed of light, and $\gamma \in \mathbb{R}^+$ captures the path loss exponent depending on the communication environment. Based on

Eq. *(1)-(3)*, the overall expected path loss is derived as follows:

$$\mathcal{P}(z_{gNB}, d_{n,gNB}) = Pr^{LoS}\mathcal{P}_{LoS} + (1 - Pr^{LoS})\mathcal{P}_{NLoS} \quad (4)$$

Each RIS consists of a uniform linear array with $\mathcal{E} = \{1, \dots, e, \dots, |\mathcal{E}|\}$ reflecting elements and $\omega_e \in [0, 2\pi)$ denotes each element's phase shift of the reflection. Also, we consider that the amplitude of the reflection coefficient is 1 and the RIS is placed at a height $z_r[m]$. For each RIS r, the corresponding diagonal reflection matrix is $\Omega_r = diag(e^{j\omega_1}, \dots, e^{j\omega_{|\mathcal{E}|}})$ and the first RIS element acts as the reference point for the rest of the calculations. Also, we consider that all the deployed RISs have the same structure.

Based on Eq. *(4)*, we can determine the channel gain $g_{n,gNB}$ of the direct communication link between the IoT node n and the gNB/MEC server as follows:

$$g_{n,gNB} = \sqrt{\frac{1}{\mathcal{P}(z_{gNB}, d_{n,gNB})}} \cdot \tilde{g}, \quad (5)$$

where $\tilde{g} \backsim \mathcal{CN}(0,1)$ is a random variable following the complex Gaussian distribution with $m_{\tilde{g}} = 0$ and $\sigma^2_{\tilde{g}} = 1$ and it captures the transmitted signal's scattering.

Focusing on the link between the IoT node and each RIS r, the channel gain coefficient is derived as follows:

$$\mathbf{g}_{n,r} = \sqrt{\frac{1}{\mathcal{P}_{n,r}}}[1, e^{-j\frac{2\pi}{\lambda}\delta\phi_{n,r}}, \dots, e^{-j\frac{2\pi}{\lambda}(|\mathcal{E}|-1)\delta\phi_{n,r}}]^T, \quad (6)$$

where $\mathbf{g}_{n,r} \in \mathbb{C}^{|\mathcal{E}|\times 1}$, $\mathcal{P}_{n,r} = \zeta(d_{n,r})^{\gamma'}$, ζ is the path loss among the node n and the RIS $\mathcal{R}_r$ at the reference point of 1m, $d_{n,r}$ is the distance among the node n and the RIS r, $\lambda[m]$ is the carrier signal's wavelength, δ is the antenna separation, and $\phi_{n,r}$ represents the cosine of the arrival angle of the node's n transmitted signal at the RIS r.

Focusing on the communication between each RIS $\mathcal{R}_r$ and the gNB/MEC server, the channel gain $\mathbf{g}_{r,gNB} \in \mathbb{C}^{|\mathcal{E}|\times 1}$ is:

$$\mathbf{g}_{r,gNB} = \sqrt{\frac{1}{\mathcal{P}_{r,gNB}}}\left(\sqrt{\frac{\kappa}{1+\kappa}}\mathbf{g}^{LoS}_{r,gNB} + \sqrt{\frac{1}{1+\kappa}}\mathbf{g}^{NLoS}_{r,gNB}\right), \quad (7)$$

where $\mathcal{P}_{r,gNB} = \mathcal{P}(z_{gNB} - z_r, d_{r,gNB})$ denotes the path loss of the link, κ represents the Rician factor and $\mathbf{g}^{LoS}_{r,gNB} = [1, e^{-j\frac{2\pi}{\lambda}\delta\phi_{r,gNB}}, \dots, e^{-j\frac{2\pi}{\lambda}(|\mathcal{E}|-1)\delta\phi_{r,gNB}}]^T$ and $\mathbf{g}^{NLoS}_{r,gNB} \backsim \mathcal{CN}(0,1)$ capture the LoS and the NLoS components, respectively, with $\phi_{r,gNB}$ representing the cosine of the signals departure angle.

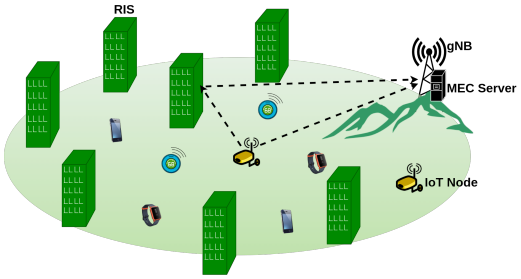

Fig. 1 – Overview of the RIS-enabled integrated communications and computing environment.

Combining all the above, we can derive the total channel gain as follows:

$$G_n = |g_{n,gNB} + \sum_{\forall r\in\mathcal{R}} \mathbf{g}^H_{r,gNB}\Omega_r\mathbf{g}_{n,r}|^2. \quad (8)$$

Without loss of generality, we consider $G_1 \leq \dots \leq G_n \leq \dots \leq G_{|N|}$. The Non-Orthogonal Multiple Access (NOMA) technique is adopted to facilitate the IoT node to offload its computing task's data to the MEC server, while ensuring high bandwidth utilization efficiency. Also, the Successive Interference Cancellation (SIC) technique is applied at the receiver to further mitigate the interference sensed by each node [25]. Thus, each node's achieved data rate is:

$$\mathrm{R}_n = W\log_2(1 + \frac{G_nP_n}{\sum_{n'=1}^{n-1} G_{n'}P_{n'} + I_0})[bps], \quad (9)$$

where $W[Hz]$ is the system's bandwidth, and I_0 is power of the Additive White Gaussian Noise (AWGN).

2.2 Overview of location-aware task offloading framework

In the following, we provide an overall overview of the proposed location-aware task offloading framework, by presenting each component, while also highlighting their interactions and the information and control flow among the different components. The first two main components serve as the enablers for the energy efficient task offloading, from the perspective of location-awareness and improved communication environment. Those two components provide input to the third one in order to perform the sophisticated decision-making of the energy efficient task offloading process.

Initially, an artificial intelligent method is introduced based on a Reinforcement Learning (RL) model and the RIS technology, to enable each IoT node to accurately determine its position. It is noted that at least four signals are needed in order to accurately predict a node's position. Specifically, each node selects a set of three RISs based on a low-complexity RL model. Then, based on the signal stemming from the gNB and the reflected signals

on the three selected RISs, each node determines its position in a distributed manner following a Least Square Algorithm [26]. Thus, each node can also determine its distance from the gNB/MEC server. *Second*, the optimal phase shifts of each RIS's elements are determined aiming at maximizing the total received signal strength from the nodes, thus partially controlling the radio propagation conditions. This approach enables the nodes to ultimately decrease their uplink transmission power, thus, contributing to the energy efficient transmission of the node's data to the MEC server for further processing. *Third*, a contract-theoretic task offloading framework is developed enabling the MEC server to provide personalized rewards to the nodes in order to offload their data to it, instead of consuming their limited energy for processing them locally on their devices. The MEC server learns the nodes' communications and computing characteristics, while interacting with them, in order to provide optimal rewards following the principles of contract theory. The optimal effort of the nodes, consisting of their optimal uplink transmission power, and their offloaded data to the MEC server, is also determined. In the following sections, a detailed analysis of the components' operation is provided.

3. RIS-ENABLED PNT SERVICES

In this section, we introduce a novel PNT solution to enable each node to distributedly and accurately determine its position. Four signals are needed to perform the multilateration and determine the node's position. One signal stems from the gNB's periodic transmissions, while the rest of the three signals can be derived by the reflected signals at three strategically selected RISs by the IoT node. An indicator that quantifies the node's accurate position calculation is the Geometric Dilution of Precision (GDOP). The GDOP indicates the success of the RISs' geometric constellation to accurately determine the node's position, while a low $GDOP$ value concludes to better ac- curacy. Based on the existing literature, the lowest re- ported $GDOP$ value is 1.5811, as derived by the GNSS with four satellites [27].

The set of possible RISs strategies is denoted as $\mathcal{S} = \{s_1, \dots, s_s, \dots, s_{|\mathcal{S}|}\}$, where $s_s = \{\mathcal{R}_i, \mathcal{R}_j, \mathcal{R}_r\}$, $i \neq j \neq r$, $\mathcal{R}_i, \mathcal{R}_j, \mathcal{R}_r \in \mathcal{R}$. Each node can select a RISs strategy (i.e., triplet of RISs), which will result to a corresponding $GDOP\,(s_s)$. Thus, we define the reward that the node experiences by selecting a strategy, as: $f(s_s) = \frac{1.5811}{GDOP(s_s)}$. An RL model is introduced based on the gradient ascent algorithms to enable each node to autonomously select a strategy of three RISs to determine its position. Specifically, the IoT nodes act as learning automata and they probabilistically learn to either select the same strategy (Eq. (10)a) or a different one (Eq. (10)b) based on the received reward.

$$P(s_s^{(i+1)}) = P(s_s^{(i)}) + \mu_1 f(s_s^{(i)})(1 - P(s_s^{(i)})) - \mu_2(1 - f(s_s^{(i)})P(s_s^{(i)}), \text{ if } s_s^{(i+1)} = s_s^{(i)} \quad \textit{(10)}\text{a}$$

$$P(s_s^{(i+1)}) = P(s_s^{(i)}) - \mu_1 f(s_s^{(i)})P(s_s^{(i)}) + \mu_2(1 - f(s_s^{(i)}))(\frac{1}{|\mathcal{S}| - 1} - P(s_s^{(i)})), \text{ if } s_s^{(i+1)} \neq s_s^{(i)} \quad \textit{(10)}\text{b}$$

where i denotes the iteration of the RL algorithm, and $\mu_1, \mu_2 \in [0, 1]$ are the learning parameters. For large values of μ_1, the node performs extensive exploration of its available strategies, thus, the RL algorithm converges slowly. In our approach, we consider $\mu_2 = 0$, implementing the Linear Reward-Inaction (LRI) algorithm, and enabling the target to probabilistically select the strategy with the highest reward, without performing an exhaustive exploration. After convergence of the RL algorithm is achieved, i.e., when the probability of choosing one strategy is close to one, the node has determined its RISs selection. The node's position is determined following the *Least Square Algorithm (LSA)* [26]. Specifically, each node can measure the four pseudoranges based on the four received signals from the gNB and the three selected RISs, as follows:

$$r_{gNB,t} = |\mathbf{r}_t - \mathbf{r}_{gNB}| - \Delta t \cdot c \quad \textit{(11)}$$

$$r_{gNB,R_i,t} = \mathbf{1}_{gNB,R_i}(\mathbf{r}_{R_i} - \mathbf{r}_{gNB}) + \mathbf{1}_{R_i}(\mathbf{r}_t - \mathbf{r}_{R_i}) - \Delta t \cdot c \quad \textit{(12)}$$

$$r_{gNB,R_j,t} = \mathbf{1}_{gNB,R_j}(\mathbf{r}_{R_j} - \mathbf{r}_{gNB}) + \mathbf{1}_{R_j}(\mathbf{r}_t - \mathbf{r}_{R_j}) - \Delta t \cdot c \quad \textit{(13)}$$

$$r_{gNB,R_r,t} = \mathbf{1}_{gNB,R_r}(\mathbf{r}_{R_r} - \mathbf{r}_{gNB}) + \mathbf{1}_{R_r}(\mathbf{r}_t - \mathbf{r}_{R_r}) - \Delta t \cdot c \quad \textit{(14)}$$

where Δt denotes the gNB's and the node's time clock offsets. We set Eq. *(11) - (14)* equal to zero and we derive the corresponding functions $h_1 - h_4$, where the four unknown variables are x_n, y_n, z_n and Δt. We solve the algebraic system and determine the values $\mathfrak{r}_n^{(i'=1)} = (x_n^{(i'=1)}, y_n^{(i'=1)}, z_n^{(i'=1)})$ and $\Delta t^{(i'=1)}$, where i' denotes the iteration of the Least Square Algorithm. Then, we determine the Jacobian (Eq. *(15)*) and Residual (Eq. *(16)*) matrices, by setting $\zeta^{(ite')} = (x_n^{(i'=1)}, y_n^{(i'=1)}, z_n^{(i'=1)}, \Delta t^{(i'=1)})$.

$$\mathcal{J}^{(ite')} = \begin{bmatrix} \frac{\partial h_1}{\partial x_n}(\zeta^{(i')}) & \frac{\partial h_1}{\partial y_n}(\zeta^{(i')}) & \frac{\partial h_1}{\partial z_n}(\zeta^{(i')}) & \frac{\partial h_1}{\partial \Delta t}(\zeta^{(i')}) \\ \frac{\partial h_2}{\partial x_n}(\zeta^{(i')}) & \frac{\partial h_2}{\partial y_n}(\zeta^{(i')}) & \frac{\partial h_2}{\partial z_n}(\zeta^{(i')}) & \frac{\partial h_2}{\partial \Delta t}(\zeta^{(i')}) \\ \frac{\partial h_3}{\partial x_n}(\zeta^{(i')}) & \frac{\partial h_3}{\partial y_n}(\zeta^{(i')}) & \frac{\partial h_3}{\partial z_n}(\zeta^{(i')}) & \frac{\partial h_3}{\partial \Delta t}(\zeta^{(i')}) \\ \frac{\partial h_4}{\partial x_n}(\zeta^{(i')}) & \frac{\partial h_4}{\partial y_n}(\zeta^{(i')}) & \frac{\partial h_4}{\partial z_n}(\zeta^{(i')}) & \frac{\partial h_4}{\partial \Delta t}(\zeta^{(i')}) \end{bmatrix} \quad \textit{(15)}$$

$$\mathcal{R}es^{(i')} = \begin{bmatrix} h_1(\zeta^{(i')}) \\ h_2(\zeta^{(i')}) \\ h_3(\zeta^{(i')}) \\ h_4(\zeta^{(i')}) \end{bmatrix} \quad (16)$$

The nodes' position and the clock's offset are determined by solving the least square problem, as $(\Delta x_n, \Delta y_n, \Delta z_n, \Delta(\Delta t)) = (\mathcal{J}^{(i')T} \cdot \mathcal{J}^{(i')})^{-1} \cdot \mathcal{J}^{(i')T} \cdot \mathcal{R}es^{(i')}$ and a new estimate is determined as $\zeta^{(i'+1)} = (x_n^{(i')} + \Delta x_n, y_n^{(i')} + \Delta y_n, z_n^{(i')} + \Delta z_n, \Delta t^{(i')} + \Delta(\Delta t))$. The LSA is repeated iteratively until the point-wise difference of the estimates between two consecutive iterations are sufficiently small. Based on the final estimate of $\zeta^{(i')}$, the GDOP value is estimated as $GDOP = (\mathcal{J}^{(i')T} \cdot \mathcal{J}^{(i')})^{-1}$ and provided as input to the RL algorithm to enable the nodes' RISs selection.

4. RIS ELEMENTS' PHASE SHIFTS OPTIMIZATION

In this section, we study the optimization of the RISs' phase shifts towards maximizing the overall signal strength received by the nodes to the gNB, while the signals are being reflected at each RIS. We denote as $\omega_r = [\omega_1, \dots, \omega_e, \dots, \omega_{|\mathcal{E}|}]$ the phase shifts vector of each RIS r. Thus, the corresponding optimization problem for the nodes signals reflected at each RIS is formulated as follows:

$$\max_{\{\omega_r\}_{\forall r \in R}} \sum_{n=1}^{|N|} |g_{n,gNB} + \sum_{\forall r \in \mathcal{R}} \mathbf{g}_{r,gNB}^H \Omega \mathbf{g}_{n,r}|^2 \quad (17)\text{a}$$

$$\text{s.t.} \quad 0 \leq \omega_e < 2\pi, \forall e \in \mathcal{E} \quad (17)\text{b}$$

Towards addressing the optimization problem ((*17)*a) - ((*17)*b), we set $\upsilon_e = e^{j\omega_e}, \forall e \in \mathcal{E}$, and we have the corresponding vector $\upsilon_r = [\upsilon_1, \dots, \upsilon_e, \dots, \upsilon_{|\mathcal{E}|}] \in \mathbb{C}^{|\mathcal{E}| \times 1}$. By setting $\hat{\mathbf{g}}_{n,r}^H = \mathbf{g}_{r,gNB}^H \cdot diag(\mathbf{g}_{n,r}) \in \mathbb{C}^{1 \times |\mathcal{E}|}$, we can rewrite the optimization problem (Eq. *(17)*a) - ((*17)*b), as follows.

$$\max_{\{\upsilon_r\}_{\forall r \in R}} \sum_{n=1}^{|N|} |g_{n,gNB} + \sum_{\forall r \in \mathcal{R}} \hat{\mathbf{g}}_{n,r}^H \upsilon|^2 \quad (18)\text{a}$$

$$\text{s.t.} \quad |\upsilon_e| = 1, \forall e \in \mathcal{E} \quad (18)\text{b}$$

It is easily observed that the optimization problem (Eq. *(18)*a) - ((*18)*b) is non-concave, as both the objective function (Eq. *(18)*a) is non-concave with respect to υ_r, and the constraint (Eq. *(18)*b) defines a non-convex set. Therefore, in the following analysis, we introduce a low-complexity heuristic approach to determine υ_r and correspondingly the RISs' phase shifts $\omega_r, \forall r \in \mathcal{R}$.

Initially, we observe that in a multi-nodes scenario, the optimal phase shifts of the RISs elements are in general different for each transmitting node. Thus, we need to design a method to determine the optimal phase shifts that will simultaneously improve the channel gain of all the nodes. Initially, we consider the simple scenario of one node residing in the system. In this case, the direct signal to the gNB should be perfectly aligned with the reflected signals at each RIS's elements. Thus, we can derive the optimal phase shifts ω_r^* for each RIS as follows: $\angle g_{1,gNB} = -\angle \hat{\mathbf{g}}_{1,r} + \angle \upsilon_r \Leftrightarrow \angle \upsilon_r = \angle g_{1,gNB} + \angle \hat{\mathbf{g}}_{1,r}$.

Generalizing the above outcome to a multi-nodes scenario, and denoting $\upsilon_r^{(n)} = [\upsilon_1^{(n)}, \dots, \upsilon_e^{(n)}, \dots, \upsilon_{|\mathcal{E}|}^{(n)}] \in \mathbb{C}^{|\mathcal{E}| \times 1}$ for each node, we conclude to the following optimal outcome for each node n that its signal is reflected to a RIS r: $\upsilon_r^{(n)} = e^{j\angle g_{n,gNB}} e^{j\angle \hat{\mathbf{g}}_{n,r}}, \forall n \in N$. We observe that the optimal phase shifts for each node are different. Therefore, in order to holistically accommodate all the nodes' signals transmission characteristics, we introduce a weighted summation of their individual $\upsilon_r^{(n)}$ values, as follows: $\upsilon = \sum_{n=1}^{|N|} w_n \upsilon_r^{(n)}$, with $\sum_{n=1}^{|N|} w_n = 1$. Therefore, the optimization problem (Eq. *(18)*a) - ((*18)*b) can be rewritten as follows:

$$\max_{\mathbf{w}} \sum_{n=1}^{|N|} |g_{n,gNB} + \mathbf{g}_{r,gNB}^H \Omega \mathbf{g}_{n,r}|^2 \quad (19)\text{a}$$

$$\text{s.t.} \quad 0 \leq w_n \leq 1, \forall n \in N \quad (19)\text{b}$$

$$\sum_{n=1}^{|N|} w_n = 1. \quad (19)\text{c}$$

where $\Omega_r = diag(e^{j\angle \upsilon})$ and $\mathbf{w} = [w_1, \dots, w_n, \dots, w_{|N|}]$. The optimization problem (Eq. *(19)*a) - ((*19)*c) consists of a non-negative linear objective function and constraints, thus, it can be solved based on standard optimization tools, and the optimal weights $\mathbf{w}^*$ can be determined. Thus, we can determine the optimal RISs elements' phase shifts $\omega_r^*, \forall r \in \mathcal{R}$.

5. CONTRACT-THEORETIC ENERGY EFFICIENT DATA OFFLOADING

In this section, we introduce a novel contract-theoretic task offloading mechanism to enable the IoT nodes to process their computing tasks in an energy efficient manner. Following the principles of contract theory, the MEC server offers personalized rewards to the nodes, in order for the latter ones to offload their computing task's data to the MEC server in an energy efficient manner. Each node is characterized by its personal communications and computing characteristics. Based on this observation, we define the IoT node's n type, as $t_n = \frac{G_n}{d_{n,gNB}} \cdot \frac{B_n}{\phi_n}$. The physical meaning of the node's type reflects the potential of the node to offload a large amount of data to the MEC server in an energy efficient manner, i.e., with low transmission power levels. A large value of the node's

type represents a node that is close to the MEC server, is characterized by improved channel gain, and can offload a large amount of non-computationally intensive data. For presentation purposes, we map the node's type in the interval $t_n \in [0, 1]$.

The nodes' types are private information and the MEC server estimates them probabilistically (incomplete information) via a Probability Density Function (PDF) $f(t)$, with cumulative distribution function $F(t)$. The MEC server's PDF can be derived and dynamically adapted based on the MEC server's interactions with the nodes. In contrast, in a benchmarking scenario, the MEC server deterministically knows the nodes' types. Considering the energy efficient operation of the system, each node should offload its data with low transmission power not only to save its own energy, but also to avoid increasing the interference. Also, each node should be incentivized to offload its computing task's data to avoid processing them locally and consuming its device's energy. Thus, we define the effort $q(t_n)$ that each node can contribute to the energy efficient operation of the system as $\frac{B_n}{P_n}$, and by making the mapping $[0, \frac{B_n}{P_n}] \rightarrow [0, 1], \forall n \in N$, we have $q(t_n) \in [0, 1]$. It is noted that the node's effort $q(t_n)$ is a strictly increasing function of its type, as a node with improved communications and favorable computing characteristics (e.g., low computationally intensive data) can contribute more to the system's energy efficient operation.

The MEC server aims to incentivize the IoT nodes to operate in an energy efficient manner by providing personalized rewards accounting for their communications and computing characteristics. The personalized rewards are defined as $r(t_n) = t_n \cdot q(t_n)$, and depend on the node's type and its corresponding provided effort $q(t_n)$ to the energy efficient operation of the system. It is noted that in a real-life implementation the rewards can be mapped to correspondingly proportional computing capacity that the MEC server allocates to the nodes in order to remotely process their computing tasks' data. Therefore, each node's utility from offloading and processing its data at the MEC server is derived as follows.

$$U_n(t_n, q(t_n), r(t_n)) = t_n \mathfrak{e}(r(t_n)) - \mathfrak{c} \cdot q(t_n) \qquad (20)$$

where $\mathfrak{c} \in \mathbb{R}^+$ denotes the nodes' cost to provide their effort $q(t_n)$ and $\mathfrak{e}(r(t_n))$ denotes the nodes' evaluation function in terms of assessing the received rewards from the MEC server. The evaluation function is concave and strictly increasing with respect to the reward capturing the increasing satisfaction of the nodes from receiving a higher reward. Thus, the node's utility reflects the node's overall satisfaction accounting for its invested effort and the received rewards.

Focusing on the MEC server's benefits, (and respectively, the benefits of the service provider), the MEC server's utility can be structured as follows.

$$U_{MEC}(\mathbf{t}) = \int_0^1 f(t)[q(t) - \mathrm{c}r(t)]dt \qquad (21)$$

where $\mathrm{c} \in \mathbb{R}^+$ denotes the MEC server's cost to provide the rewards and $\mathbf{t} = \{t_n\}_{\forall n \in N}$. The physical meaning of the MEC server's utility is its (unitless) profit/benefit from incentivizing the nodes to operate in an energy efficient manner. The MEC server probabilistically estimates the nodes' types based on the PDF $f(t)$, thus, the nodes' indices are omitted in Eq. *(21)*.

Towards determining the nodes' optimal effort and rewards, the principles of contract theory are adopted [28]. The MEC server provides a personalized contract $\{r(t_n), q(t_n)\}$ to each node, considering each node's invested effort $q(t_n)$. The provided contract should respect the conditions of Individual Rationality (IR) and Incentive Compatibility (IC) in order to be feasible and accepted by each node.

Definition 1. *Each IoT node's utility should be non-negative, i.e.,* $U_n(t_n, q^*(t_n), r^*(t_n)) \geq 0$ *for the optimal contract* $\{r^*(t_n), q^*(t_n)\}$ *under the individual rationality condition.*

Definition 2. *An optimal contract* $\{r^*(t_n),\ q^*(t_n)\}$ *is incentive compatible, if each node achieves the highest utility as compared to any other contract designed for another node of different type* t'*, i.e.,* $t\mathfrak{e}(r^*(t)) - \mathfrak{c}q^*(t) \geq t\mathfrak{e}(r^*(t')) - \mathfrak{c}q^*(t')$.

The MEC server aims at maximizing its achieved utility while guaranteeing the nodes appropriate incentivization via the IR and IC conditions. Thus, the corresponding optimization problem in order to determine the optimal contracts among the MEC server and the IoT nodes is formulated as follows.

$$\max_{\{r(t), q(t)\}_{\forall t \in [0,1]}} \int_0^1 f(t)[q(t) - \mathrm{c}r(t)]dt \qquad (22)\text{a}$$

$$\text{s.t.} \quad t\mathfrak{e}(r(t)) - \mathfrak{c} \cdot q(t) \geq 0, \forall t \in [0, 1] \quad \text{(IR)} \qquad (22)\text{b}$$

$$t\mathfrak{e}(r^*(t)) - \mathfrak{c}q^*(t) \geq t\mathfrak{e}(r^*(t')) - \mathfrak{c}q^*(t'), \forall t \neq t' \quad \text{(IC)} \qquad (22)\text{c}$$

The optimization problem (Eq. *(22)*a) – (*(22)*c) is non-convex due to the form of the objective function and its constraints. Towards addressing this problem, we reduce its constraints.

Theorem 1 (Reduction of IR Constraints). *The IR constraints can be reduced to* $t_{min}\mathfrak{e}(r(t_{min})) - \mathfrak{c} \cdot q(t_{min}) = 0$*, with* $t_{min} \rightarrow 0^+$*, if the IC constraints hold true.*

Proof. If the IC constraints hold true, we have $t\mathfrak{e}(r(t)) - \mathfrak{c}q(t) \geq t\mathfrak{e}(r(t_{min})) - \mathfrak{c}q(t_{min}) \geq t_{min}\mathfrak{e}(r(t_{min})) -$

$\mathfrak{c}q(t_{min})$, given that $t \geq t_{min}$ and $\mathfrak{e}(\cdot)$ is a strictly increasing function with respect to t. Also, it holds true that $t_{min}\mathfrak{e}(r(t_{min})) - \mathfrak{c}q(t_{min}) = 0$, given that the MEC server will provide just the sufficient and necessary rewards, to the IoT nodes in order to contribute to the system's energy efficient operation. □

Based on Theorem 1, the IR constraints are reduced. In the following theorem, we further reduce the IC constraints.

Theorem 2 (Reduction of IC Constraints). *The IC constraints can be reduced to the following two constraints (i)* $r'(t) \geq 0$ *(monotonicity), (ii)* $t \cdot r'(t) \cdot \mathfrak{e}'(r(t)) = \mathfrak{c}q'(t)$ *(local incentive compatibility), if the Spence-Mirrlees condition [28]* $\frac{\partial}{\partial t}[-\frac{\frac{\partial U_n}{\partial r}}{\frac{\partial U_n}{\partial q}}] > 0$ *holds true for each node's utility.*

Proof. Based on Eq. *(20)*, we have $\frac{\partial U_n}{\partial q} = -\mathfrak{c} < 0$, as $\mathfrak{c} \in \mathbb{R}^+$ and $\frac{\partial U_n}{\partial r} = t\frac{\partial \mathfrak{e}(r(t))}{\partial r} > 0$, as $\mathfrak{e}(r(t))$ is a strictly increasing function with respect to $r(t)$ and $t \in [0,1]$. Thus, we have $\frac{\partial^2 U_n}{\partial t \partial r} = \frac{\partial \mathfrak{e}(r(t))}{\partial r} + t\frac{\partial^2 \mathfrak{e}(r(t))}{\partial t \partial r}[q(t) + t\frac{\partial q(t)}{\partial t}] > 0$, given that $\mathfrak{e}(r(t))$, $r(t)$, and $q(t)$ are strictly increasing functions with respect to t, and $\mathfrak{e}(r(t))$ is a concave function with respect to t. Therefore, the Spence - Mirrlees condition holds true. Then, we check the necessity and sufficiency of the monotonicity and Local Incentive Compatibility (LIC) constraints. First, we show that the latter two conditions hold true, if the IC constraints hold true. Given that the IC constraints hold true, we have $t\mathfrak{e}(r(t)) - \mathfrak{c}q(t) \geq t\mathfrak{e}(r(t')) - \mathfrak{c}q(t') \Leftrightarrow U_n(t, q(t), r(t)) \geq U_n(t, q(t'), r(t')), \forall t \neq t'$. This means that the value $U_n(t, q(t), r(t))$ is the optimal one for the node of type t, thus, the following hold true: $\frac{\partial U_n(t,r(t'),q(t'))}{\partial t'}|_{t'=t} = 0$ and $\frac{\partial^2 U_n(t,r(t'),q(t'))}{\partial t'^2}|_{t'=t} \leq 0$. Based on $\frac{\partial U_n(t,r(t'),q(t'))}{\partial t'}|_{t'=t} = 0$, we have $tr'(t')\mathfrak{e}'(r(t')) = \mathfrak{c}q'(t')$, thus, the local incentive compatibility condition holds true for $t' = t$. Based on $\frac{\partial^2 U_n(t,r(t'),q(t'))}{\partial t'^2}|_{t'=t} \leq 0$ we have $tr''(t')\mathfrak{e}'(r(t')) + t(r'(t'))^2 e''(r(t')) \leq \mathfrak{c}q''(t')$ and by differentiating the equation $\frac{\partial U_n(t,r(t'),q(t'))}{\partial t'}|_{t'=t} = 0$ with respect to t, we have $\mathfrak{c}q''(t') = r'(t')\mathfrak{e}'(r(t')) + tr''(t')\mathfrak{e}'(r(t')) + t(r'(t'))^2\mathfrak{e}''(r(t'))$. Therefore, we have $r'(t')\mathfrak{e}'(r(t')) \geq 0$, and we know that $\mathfrak{e}'(r(t')) > 0$ given that $\mathfrak{e}(\cdot)$ is a strictly increasing function. Therefore, we conclude that $r'(t') \geq 0$ for $t' = t$, showing that the monotonicity condition holds true. By following the reduction at absurdity approach, we show that the IC constraints hold true, if the monotonicity and the LIC constraints hold true. Assuming that the IC constraints are not valid, we have: $t\mathfrak{e}(r(t)) - \mathfrak{c}q(t) < t\mathfrak{e}(r(t')) - \mathfrak{c}q(t') \Leftrightarrow \int_t^{t'} [tr'(x)\mathfrak{e}'(r(x)) - \mathfrak{c}q'(x)]dx > 0$. We integrate the LIC condition, and we have: $\int_t^{t'} [tr'(x)\mathfrak{e}'(r(x)) - \mathfrak{c}q'(x)]dx = 0$. From the monotonicity condition, we have $t < x < t' \overset{r'(x)\geq 0}{\Leftrightarrow} tr'(x) < xr'(x) \overset{\mathfrak{e}'(r(x))>0}{\Leftrightarrow} tr'(x)\mathfrak{e}'(r(x)) < xr'(x)\mathfrak{e}'(r(x)) \Leftrightarrow tr'(x)\mathfrak{e}'(r(x)) - \mathfrak{c}q'(x) < xr'(x)\mathfrak{e}'(r(x)) - \mathfrak{c}q'(x) \Leftrightarrow \int_t^{t'} [tr'(x)\mathfrak{e}'(r(x)) - \mathfrak{c}q'(x)]dx < \int_t^{t'} [xr'(x)\mathfrak{e}'(r(x)) - \mathfrak{c}q'(x)]dx \Leftrightarrow \int_t^{t'} [tr'(x)\mathfrak{e}'(r(x)) - \mathfrak{c}q'(x)]dx < 0$. Thus, there is a contradiction, and, the IC constraints hold true. □

Based on theorems 1 and 2, the optimization problem (Eq.*(22)*a) - (*(22)*c) can be rewritten as follows:

$$\max_{\substack{\{r(t),q(t)\}\\ t\in[0,1]}} \int_0^1 f(t)[q(t) - \mathsf{c}r(t)]dt \qquad (23)\text{a}$$

$$\text{s.t.} \quad t_{min}\mathfrak{e}(r(t_{min})) - \mathfrak{c}q(t_{min}) = 0, t_L \to 0^+ \qquad (23)\text{b}$$

$$r'(t) \geq 0 \qquad (23)\text{c}$$

$$tr'(t)\mathfrak{e}'(r(t)) = \mathfrak{c}q'(t), \forall t \in [0,1] \qquad (23)\text{d}$$

Following the approach introduced by Mirrlees [28], we initially solve the above optimization problem considering only the constraints (*(23)*b) and (*(23)*d), and subsequently we check if the derived solution satisfies the monotonicity constraint (*(23)*c). Towards this direction, we define the function: $W(t) = t\mathfrak{e}(r(t)) - \mathfrak{c}q(t) = \max_{t'}\{t\mathfrak{e}(r(t')) - \mathfrak{c}q(t')\}$ and we have $\frac{\partial W(t)}{\partial t}|_{t=t'} = \mathfrak{e}(r(t))$. Then, we integrate the latter expression and we get $W(t) = \int_{t_{min}}^t \mathfrak{e}(r(x))dx + W(t_{min}), t_{min} \to 0^+$. It is noted that for $t_{min} \to 0^+$, the IR constraint for the IoT node with the lowest type is binding. Therefore, we get $W(t_{min}) = 0$ and $W(t) = \int_{t_{min}}^t \mathfrak{e}(r(x))dx$. Thus, we have $q(t) = \frac{1}{\mathfrak{c}}t\mathfrak{e}(r(t)) - \frac{1}{\mathfrak{c}}W(t)$ and the MEC server's utility (Eq. *(21)*) is rewritten as follows: $U_{MEC}(\mathbf{t}) = \int_0^1 f(t)[\frac{1}{\mathfrak{c}}t\mathfrak{e}(r(t)) - \frac{1}{\mathfrak{c}}W(t) - \mathsf{c}r(t)]dt = \int_0^1 f(t)[\frac{1}{\mathfrak{c}}t\mathfrak{e}(r(t)) - \frac{1}{\mathfrak{c}}\int_0^t \mathfrak{e}(r(x))dx - \mathsf{c}r(t)]dt = \int_0^1 f(t)[\frac{1}{\mathfrak{c}}t\mathfrak{e}(r(t)) - \mathsf{c}r(t)]dt - \frac{1}{\mathfrak{c}}\int_0^1 (\int_0^t \mathfrak{e}(r(x))dx)f(t)dt$. The latter integral can be analyzed as follows: $\int_0^1 (\int_0^t \mathfrak{e}(r(x))dx)f(t)dt = \int_0^1 \Lambda(t)f(t)dt$, with $\Lambda(t) = \int_0^t \mathfrak{e}(r(x))dx$. We can further analyze the integral as: $\int_0^1 \Lambda(t)f(t)dt = [\Lambda(t)F(t)]_0^1 - \int_0^1 \Lambda'(t)F(t)dt = \Lambda(1)F(1) - \Lambda(0)F(0) - \int_0^1 \Lambda'(t)F(t)dt = \Lambda(1) - \int_0^1 \Lambda'(t)F(t)dt = \int_0^1 \mathfrak{e}(r(t))dt - \int_0^1 \mathfrak{e}(r(t))F(t)dt = \int_0^1 \mathfrak{e}(r(t))[1-F(t)]dt$, and rewrite the MEC server's utility, as: $U_{MEC}(\mathbf{t}) = \int_0^1 f(t)\{[\frac{1}{\mathfrak{c}}t\mathfrak{e}(r(t)) - \mathsf{c}r(t)] - \frac{1}{\mathfrak{c}}\mathfrak{e}(r(t))[1 - F(t)]\}dt$. Thus, we can rewrite the optimization problem (Eq.*(23)*a) - (*(23)*d) as follows.

$$\max_{r(t),t\in[0,1]} [\frac{1}{\mathfrak{c}}t\mathfrak{e}(r(t)) - \mathsf{c}r(t) - \frac{\mathfrak{e}(r(t))[1-F(t)]}{\mathfrak{c}f(t)}]f(t) \qquad (24)\text{a}$$

$$\text{s.t.} \quad t_{min}\mathfrak{e}(r(t_{min})) - \mathfrak{c}q(t_{min}) = 0, t_{min} \to 0^+ \qquad (24)\text{b}$$

$$r'(t) \geq 0 \qquad (24)\text{c}$$

$$tr'(t)\mathfrak{e}'(r(t)) = \mathfrak{c}q'(t), \forall t \in [0,1] \qquad (24)\text{d}$$

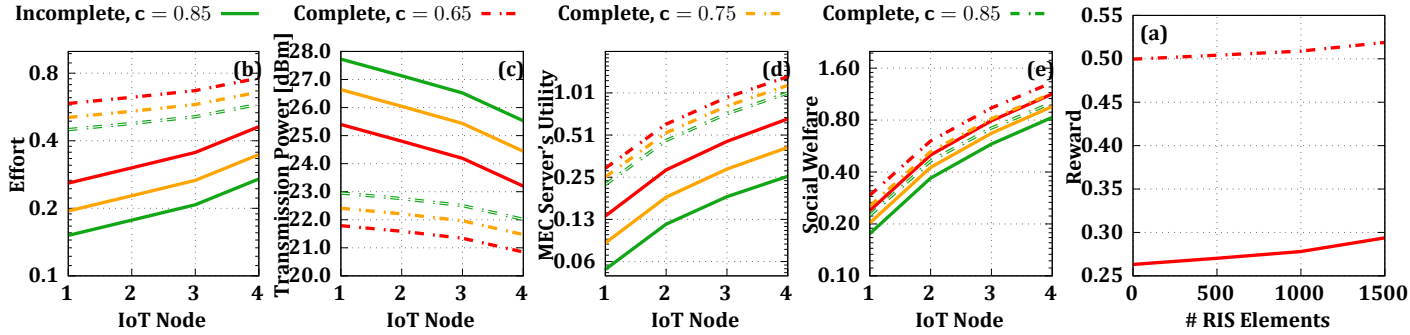

Fig. 2 – Pure operation and performance.

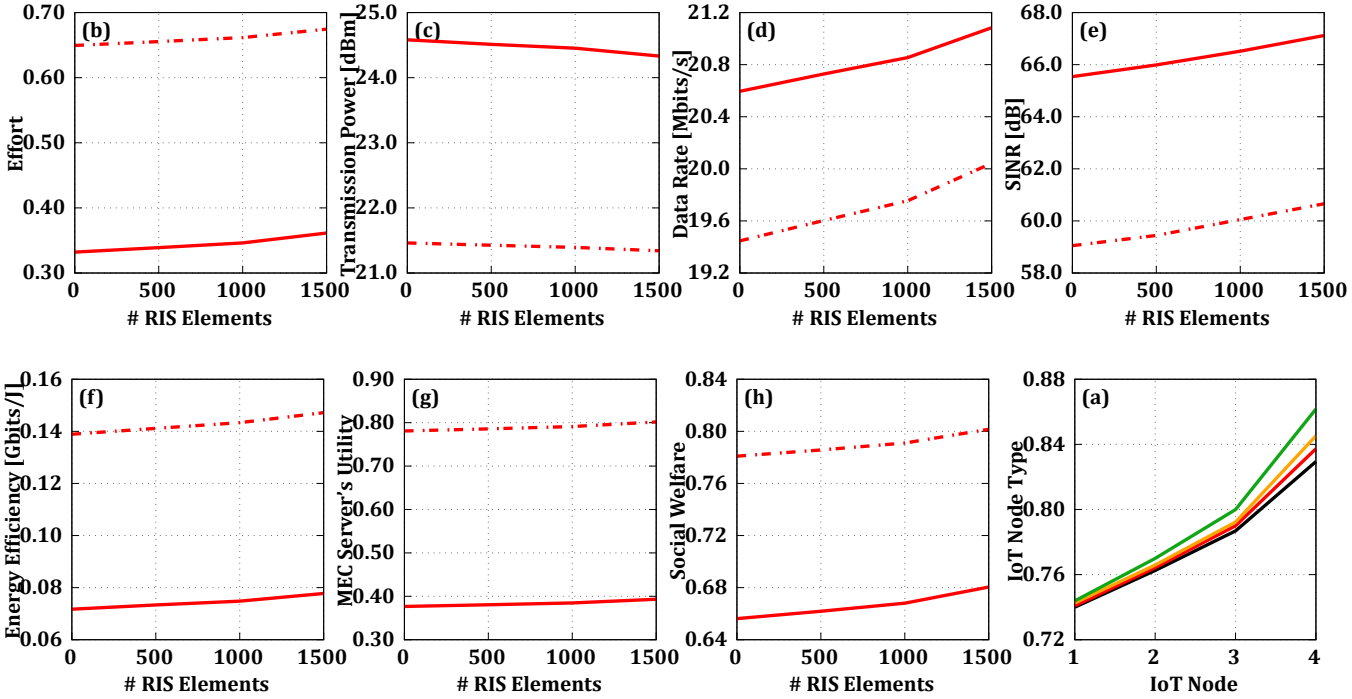

Fig. 3 – Impact of RIS technology on the system's energy efficient operation (solid line: incomplete information scenario, dotted line: complete information scenario).

In order to solve the above optimization problem, we take the first order condition of Eq. *(24)*a and we have: $\mathfrak{e}'(r(t))\frac{1}{\mathsf{c}}[t-\frac{1-F(t)}{f(t)}]=\mathsf{c}$, based on which the optimal reward $r^*(t)$ can be derived. The optimal reward $r^*(t)$ should also satisfy the monotonicity constraint. In order for the latter statement to hold true, the hazard rate $H(t)=\frac{f(t)}{1-F(t)}$ should be an increasing function with respect to the model type t. Indeed, we can easily observe that if the hazard rate $H(t)$ is an increasing function with respect to t, then the constraint (*(24)*c) holds true. By setting $g(t)=t-\frac{1-F(t)}{f(t)}$ we have $\frac{1}{\mathsf{c}}g(t)\mathfrak{e}'(r(t))=\mathsf{c}\Rightarrow r'(t)=-\frac{g'(t)\mathfrak{e}'(r(t))}{\mathsf{c}g(t)\mathfrak{e}''(r(t))}\geq 0$, as $g(t)>0$, $g'(t)=1+\frac{H'(t)}{H^2(t)}>0$, $\mathfrak{e}'(r(t))>0$ and $\mathfrak{e}''(r(t))<0$.

Concluding the analysis of determining the optimal contracts, we clarify that the hazard rate $H(t)$ is increasing with respect to t for the majority of the well-known distributions, e.g., normal, exponential, uniform. In the worst case scenario that the optimal reward $r^*(t)$ does not satisfy the monotonicity constraint, we can apply the "bunching and ironing" approach to identify the infeasible intervals $[a,b]\subseteq[0,1]$ and derive the optimal reward as $r^*(t)=\underset{r(t),t\in[0,1]}{\text{argmax}}\int_a^b[\frac{1}{\mathsf{c}}t\mathfrak{e}(r(t))-\mathsf{c}r(t)-\frac{\mathfrak{e}(r(t))[1-F(t)]}{\mathsf{c}f(t)}]f(t)dt, \forall t\in[a,b]$ [28].

6. NUMERICAL EVALUATION

In this section, we provide a detailed numerical evaluation of the proposed location-aware task offloading framework via modeling and simulation. Initially, the pure performance and operation of the proposed framework, under both scenarios of complete and incomplete information availability, is demonstrated in Section 6.1. Second, the impact of the RIS technology on the energy efficient operation of the system is studied in Section 6.2. Subsequently, the impact of our proposed PNT solution in terms of accurately determining the nodes' position and contributing to the system's energy efficient operation, is enclosed in Section 6.3. Finally, in Section 6.4 a detailed comparative evaluation of the proposed approach against alternative contract-theoretic task offloading strategies is

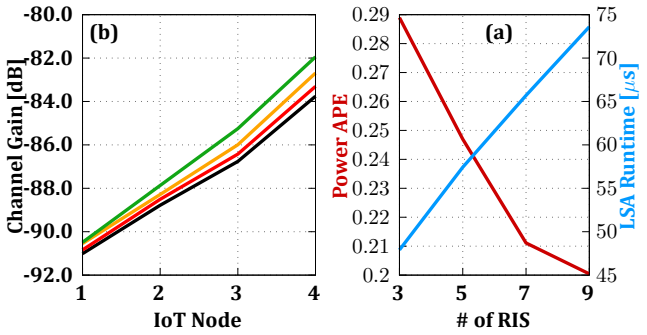

Fig. 4 – Impact of PNT solution on the system's energy efficient operation for increasing number of RIS elements (black line: no RIS, red line: 500 RIS elements, yellow line: 1000 RIS elements, green line: 1500 RIS elements).

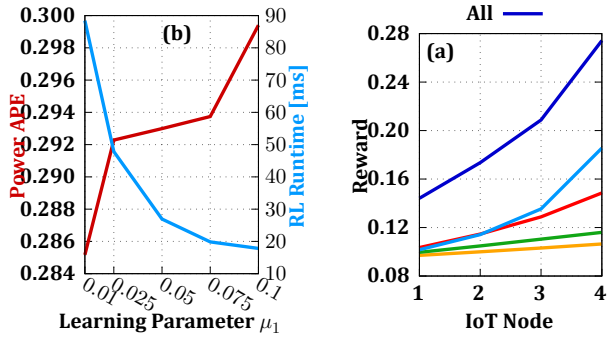

Fig. 5 – Impact of PNT solution on the system's energy efficient operation.

provided, in order to show the benefits and trade-offs of the proposed framework. The experimentation setting adopted is initialized as follows, unless otherwise explicitly stated. We consider ten RISs and four indicative IoT nodes. The gNB/MEC server's coordinates are $\mathfrak{r}_{gNB} = (100, 100, 150)$ [m]. The IoT nodes' computing tasks' characteristics are $\mathbf{B} \in [40, 50]$ Mbits, and $\phi \in [5, 10]$[MCPU Cycles/bits] and both of them follow a uniform distribution. The channel gain modeling parameters are as follows: $\alpha = 11.95$, $\beta = 0.14$, $n_{LoS} = 3dB$, $n_{NLoS} = 23dB$, $f_c = 2GHz$, $c = 3 \cdot 10^8 m/s$, $\gamma = 2$, $\zeta = 100$, $\gamma' = 2.8$, $\delta = \lambda/2$, $W = 5MHz$, $I_0 = -174dBm/Hz$. The simulation parameters for the contract-theoretic model are: $\mathfrak{c} = 0.85$, and $\mathsf{c} = [0.65, 0.75, 0.85]$. All the following presented results are derived based on a Monte Carlo analysis, averaged over 1 000 executions of each experiment.

6.1 Pure operation and performance

In this section, we demonstrate the pure operation and the inherent characteristics of the proposed task offloading framework. Figures 2a-2e present the IoT nodes reward, effort, transmission power, the MEC server's utility, and the system's social welfare, as a function of the IoT nodes. It is noted that the nodes are sorted with increasing order of their type. Also, the scenarios of complete and incomplete information of the nodes' types from the MEC server's perspective are demonstrated for different costs c for the MEC server to provide rewards. The results reveal that under the complete information scenario, the MEC server can fully exploit the communications and computing characteristics of the IoT nodes, thus, incentivizing them to provide a higher effort (Fig. 2b) via transmitting at lower power levels (Fig. 2c) and ultimately receiving higher reward (Fig. 2a). Therefore the MEC server achieves a higher utility (Fig. 2d), as well as the social welfare of the system is improved (Fig. 2e) under the complete information scenario. Moreover, the results confirm that a node of a higher type provides a higher effort (Fig. 2b) to the energy efficient operation of the system by transmitting with lower power (Fig. 2c) (please recall that the effort has an inverse proportional relation to the power), and thus getting a higher reward (Fig. 2a) from the MEC server. Furthermore, we observe that as the cost of the MEC server becomes higher in terms of providing rewards, the corresponding amount of offered rewards is decreasing (Fig. 2a) both under the complete and incomplete information scenarios. Therefore, the nodes are less incentivized to provide their effort (Fig. 2b), resulting in transmitting with higher transmission power (Fig. 2c). The latter observation concludes to a lower outcome both for the MEC server's utility and the system's social welfare (Fig. 2e).

6.2 Impact of RIS technology

In this section, we study the impact of the RIS technology on the energy efficient operation of the proposed framework and the corresponding examined edge computing system. Figures 3a-3f present the IoT nodes' reward, effort, transmission power, rate, Signal-to-Interference-plus-Noise-Ratio (SINR), energy efficiency, the MEC server's utility and the social welfare for an increasing number of RIS elements (ranging from 500 to 1500) at each RIS, under the complete and incomplete information contract-theoretic scenarios. For comparison purposes we also study a topology that is not supported by the RIS technology (i.e., 0 RIS elements), Also, figures 4a-4b demonstrate the nodes' types and channel gain as a function of the nodes' ID, respectively, for an increasing number of RIS elements. The results reveal that the RIS technology contributes to the substantial improvement of the IoT nodes' channel conditions (Fig. 4b), which contribute to the construction of a more directed beam in order to offload their data to the MEC server. Therefore, given the improved channel gain for an increasing number of RISs' elements, the nodes' types also increase (Fig. 4a), resulting in investing higher effort (Fig. 3b) by offloading their data with lower transmission power (Fig. 3c), under both the complete and incomplete scenarios. This in turn results in receiving a higher reward by the MEC server (Fig. 3a). Furthermore, given the IoT nodes' lower transmission power levels and improved channel conditions the nodes sense less interference resulting in a higher data rate (Fig. 3g) and experienced SINR

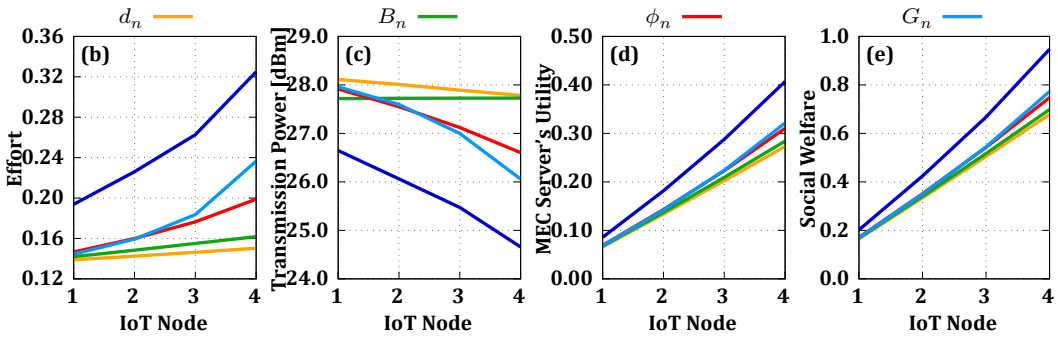

Fig. 6 – Comparative evaluation.

(Fig. 3h), and ultimately higher achieved energy efficiency (Fig. 3d). Finally, we observe that both the MEC server's utility (Fig. 3e) and the system's social welfare (Fig. 3f) increase for an increasing number of RISs elements.

6.3 Impact of PNT solution

In the following, we evaluate the impact of the RIS technology on the accuracy of the PNT solution and the resulting node's position, which in turn affects the energy efficient operation of the system. Initially, in Fig. 5a, we present the Average Percentage Error (APE) of the nodes' transmission power and the corresponding runtime of the Least Square Algorithm, when a different number of RISs are used to perform the nodes localization, e.g., 3, 5, 7, or 9 RISs (please note that 3 RISs is the minimum required number of RISs to perform localization). The results show that the APE of the nodes' transmission power decreases as the signals from more RISs are used to perform the nodes' localization, given that the nodes' position can be more accurately determined. However, the latter benefit comes at the cost of a longer execution time of the Least Square Algorithm, which considers more pseudo-ranges in order to determine the nodes' positions. Also, we study the performance of the reinforcement learning-based RISs selection by the nodes in order to determine their position. Specifically, Fig. 5b presents the APE of the nodes' transmission power and the corresponding runtime of the nodes' RL-based RISs' selection for increasing values of the learning parameter μ_1. It is noted that as the value of the learning parameter increases, the nodes explore less their RISs strategies in order to determine their position. Thus, a worse RISs choice (strategy) is performed resulting in a higher APE of the nodes' transmission power. However, given the decreased level of performed exploration by the nodes, it is observed that the corresponding convergence time of the reinforcement learning algorithm decreases.

6.4 Comparative evaluation

In this section, we provide a comparative analysis of our proposed framework against other contract-theoretic task offloading alternatives to identify its benefits and trade-offs. Five comparative scenarios are considered with respect to the definition of the IoT nodes' types, i.e., considering only the node's (i) distance $d_{n,gNB}$ from the MEC server, (ii) amount of task's data B_n, (iii) computing task's intensity ϕ_n, (iv) channel gain G_n, and (v) all previous characteristics, as introduced in this research work. Figures 6a - 6e present the IoT nodes' reward, effort, transmission power, the MEC server's utility, and the system's social welfare as a function of the IoT nodes under all the aforementioned scenarios. The results reveal that the holistic consideration of the nodes' communications and computing characteristics results in better outcomes in terms of incentivizing the nodes to provide a higher effort (Fig. 6b), thus, transmitting to the MEC server at lower power levels (Fig. 6c). Therefore, given their energy efficient operation, they receive a higher reward (Fig. 6a) from the MEC server, which correspondingly enjoys a higher utility (Fig. 6d), while also the system's social welfare (Fig. 6e) improves given its overall energy efficient operation. In contrast, the rest of the comparative scenarios present a worse performance given their myopic view regarding the IoT nodes' characteristics. Specifically, it is worth noting that the IoT nodes' channel gain characteristics become dominant in the system's performance, as they impact the energy efficient transmission of the nodes' data to the MEC server.

7. CONCLUSION

In this paper, a location-aware energy efficient task offloading mechanism in an edge computing environment is introduced, enabled by the technology of reconfigurable intelligent surfaces. Initially, a novel positioning, navigation, and timing solution supported by the RIS technology is designed to determine the IoT nodes' positions. Then, the RISs' elements optimal phase shifts are determined to optimize the IoT nodes' channel conditions in a software-defined manner, thus facilitating an energy efficient operation by decreasing their transmission power levels. Finally, a contract-theoretic model is introduced to support the nodes' energy efficient task offloading process accounting for their communications and computing characteristics. Part of our current and future work contains the extension of the proposed model in the end-to-end digital continuum, by jointly optimizing the energy efficient task offloading process to the edge, the fog, and the

core cloud options, while accounting for both the communications and computing resource availability and uncertainties.

ACKNOWLEDGMENT

The research of Mr. Hossain and Dr. Tsiropoulou was supported by the NSF CRII-1849739.

REFERENCES

[1] Xianfu Chen, Celimuge Wu, Zhi Liu, Ning Zhang, and Yusheng Ji. "Computation offloading in beyond 5g networks: A distributed learning framework and applications". In: *IEEE Wireless Communications* 28.2 (2021), pp. 56–62.

[2] Nafis Irtija, Iraklis Anagnostopoulos, Georgios Zervakis, Eirini Eleni Tsiropoulou, Hussam Amrouch, and Jörg Henkel. "Energy Efficient Edge Computing Enabled by Satisfaction Games and Approximate Computing". In: *IEEE Transactions on Green Communications and Networking* (2021).

[3] Pavlos Athanasios Apostolopoulos, Eirini Eleni Tsiropoulou, and Symeon Papavassiliou. "Cognitive Data Offloading in Mobile Edge Computing for Internet of Things". In: *IEEE Access* 8 (2020), pp. 55736–55749. DOI: 10.1109/ACCESS.2020.2981837.

[4] Gang Yang, Xinyue Xu, Ying-Chang Liang, and Marco Di Renzo. "Reconfigurable intelligent surface-assisted non-orthogonal multiple access". In: *IEEE Trans. on Wireless Communications* 20.5 (2021), pp. 3137–3151.

[5] Maria Diamanti, Maria Tsampazi, Eirini Eleni Tsiropoulou, and Symeon Papavassiliou. "Energy Efficient Multi-User Communications Aided by Reconfigurable Intelligent Surfaces and UAVs". In: *2021 IEEE International Conference on Smart Computing (SMARTCOMP)*. 2021, pp. 371–376. DOI: 10.1109/SMARTCOMP52413.2021.00075.

[6] Yali Chen, Bo Ai, Hongliang Zhang, Yong Niu, Lingyang Song, Zhu Han, and H Vincent Poor. "Reconfigurable intelligent surface assisted device-to-device communications". In: *IEEE Tr. on Wirel. Com.* 20.5 (2020), pp. 2792–2804.

[7] Jiakuo Zuo, Yuanwei Liu, and Naofal Al-Dhahir. "Reconfigurable intelligent surface assisted cooperative non-orthogonal multiple access systems". In: *IEEE Transactions on Communications* 69.10 (2021), pp. 6750–6764.

[8] Maria Diamanti, Panagiotis Charatsaris, Eirini Eleni Tsiropoulou, and Symeon Papavassiliou. "The Prospect of Reconfigurable Intelligent Surfaces in Integrated Access and Backhaul Networks". In: *IEEE Transactions on Green Communications and Networking* 6.2 (2022), pp. 859–872. DOI: 10.1109/TGCN.2021.3126784.

[9] Xiangyu Wang, Xuyu Wang, Shiwen Mao, Jian Zhang, Senthilkumar C. G. Periaswamy, and Justin Patton. "Indoor Radio Map Construction and Localization With Deep Gaussian Processes". In: *IEEE Internet of Things Journal* 7.11 (2020), pp. 11238–11249. DOI: 10.1109/JIOT.2020.2996564.

[10] Xuyu Wang, Xiangyu Wang, and Shiwen Mao. "Deep Convolutional Neural Networks for Indoor Localization with CSI Images". In: *IEEE Transactions on Network Science and Engineering* 7.1 (2020), pp. 316–327. DOI: 10.1109/TNSE.2018.2871165.

[11] Liang Yang, Fanxu Meng, Jiayi Zhang, Mazen O Hasna, and Marco Di Renzo. "On the performance of RIS-assisted dual-hop UAV communication systems". In: *IEEE Trans. on Vehicular Technology* 69.9 (2020), pp. 10385–10390.

[12] Xiaoyan Ma, Shuaishuai Guo, Haixia Zhang, Yuguang Fang, and Dongfeng Yuan. "Joint Beamforming and Reflecting Design in Reconfigurable Intelligent Surface-Aided Multi-User Communication Systems". In: *IEEE Transactions on Wireless Communications* 20.5 (2021), pp. 3269–3283.

[13] Huayan Guo, Ying-Chang Liang, Jie Chen, and Erik G Larsson. "Weighted sum-rate maximization for reconfigurable intelligent surface aided wireless networks". In: *IEEE Tr. on Wir. Comm.* 19.5 (2020), pp. 3064–3076.

[14] Chongwen Huang, Alessio Zappone, George C Alexandropoulos, Mérouane Debbah, and Chau Yuen. "Reconfigurable intelligent surfaces for energy efficiency in wireless communication". In: *IEEE Transactions on Wireless Communications* 18.8 (2019), pp. 4157–4170.

[15] Zhiyang Li, Ming Chen, Zhaohui Yang, Jingwen Zhao, Yinlu Wang, Jianfeng Shi, and Chongwen Huang. "Energy Efficient Reconfigurable Intelligent Surface Enabled Mobile Edge Computing Networks with NOMA". In: *IEEE Transactions on Cognitive Communications and Networking* (2021).

[16] Xiaoyan Hu, Christos Masouros, and Kai-Kit Wong. "Removing channel estimation by location-only based deep learning for RIS aided mobile edge computing". In: *ICC 2021*. IEEE. 2021, pp. 1–6.

[17] Xiaoyan Hu, Christos Masouros, and Kai-Kit Wong. "Reconfigurable Intelligent Surface Aided Mobile Edge Computing: From Optimization-Based to Location-Only Learning-Based Solutions". In: *IEEE Transactions on Communications* (2021).

[18] Aichen Li, Yang Liu, Ming Li, Qingqing Wu, and Jun Zhao. "Joint Scheduling Design in Wireless Powered MEC IoT Networks Aided by Reconfigurable Intelligent Surface". In: *Int. Conf. on Comm. in China*. IEEE. 2021, pp. 159–164.

[19] Xuyu Wang, Zhitao Yu, and Shiwen Mao. "Indoor localization using smartphone magnetic and light sensors: A deep LSTM approach". In: *Mobile Networks and Applications* 25.2 (2020), pp. 819–832.

[20] Xuelin Cao, Bo Yang, Chongwen Huang, Chau Yuen, Yan Zhang, Dusit Niyato, and Zhu Han. "Converged Reconfigurable Intelligent Surface and Mobile Edge Computing for Space Information Networks". In: *arXiv:2106.04248* (2021).

[21] Marco Detratti and Ferdinando Dolce. "PNT for Defense". In: *Handbook of Space Security: Policies, Applications and Programs* (2020), pp. 821–843.

[22] Sherman Lo and Yu-Hsuan Chen. "Message Design for a Robust Time Signal using Distance Measuring Equipment (DME) Pulse Pair Position Modulated (PPPM) Pseudo lite". In: *2020 European Navigation Conference (ENC)*. 2020, pp. 1–10. DOI: 10.23919/ENC48637.2020.9317492.

[23] Shuai Han, Zijun Gong, Weixiao Meng, Cheng Li, and Xuemai Gu. "Future alternative positioning, navigation, and timing techniques: A survey". In: *IEEE wireless communications* 23.6 (2016), pp. 154–160.

[24] Yiming Liu, Erwu Liu, Rui Wang, and Yuanzhe Geng. "Reconfigurable intelligent surface aided wireless localization". In: *ICC 2021-IEEE International Conference on Communications*. IEEE. 2021, pp. 1–6.

[25] Panagiotis Vamvakas, Eirini Eleni Tsiropoulou, and Symeon Papavassiliou. "Dynamic spectrum management in 5G wireless networks: A real-life modeling approach". In: *IEEE INFOCOM 2019-IEEE Conference on Computer Communications*. IEEE. 2019, pp. 2134–2142.

[26] Rabih Chrabieh, Mazen Neifer, Ganda Ouedraogo, Ines Ben Hamida, Peter Bagnall, and Serdar Sezginer. "Enhanced Multilateration Methods With A Global Approach". In: *2020 IEEE/ION Position, Location and Navigation Symposium (PLANS)*. 2020, pp. 1070–1078. DOI: 10.1109/PLANS46316.2020.9110183.

[27] Miaoyan Zhang and Jun Zhang. "A fast satellite selection algorithm: beyond four satellites". In: *IEEE Journal of Selected Topics in Signal Processing* 3.5 (2009), pp. 740–747.

[28] Patrick Bolton, Mathias Dewatripont, et al. *Contract theory*. MIT press, 2005.

AUTHORS

Md Sahabul Hossain is a Ph.D. student and research assistant in the Department of Electrical and Computer Engineering, University of New Mexico. He received his bachelor's and master's in Electrical and Electronic Engineering from the Islamic University of Technology, Bangladesh. His main research interests include distributed decision making, reinforcement learning, game theory, optimization, contract theory, and aritificial intelligence.

Nafis Irtija is a Ph.D. student and research assistant in the Department of Electrical and Computer Engineering, University of New Mexico. He received his bachelor's and master's in Electrical and Electronic Engineering from the University of Dhaka, Bangladesh. His main research interests include distributed decision making, reinforcement learning, game theory, optimization, contract theory, and prospect theory.

Maria Diamanti is a Ph.D. student and a research assistant in the School of Electrical and Computer Engineering at the National Technical University of Athens. She received her Diploma in Electrical and Computer Engineering from the Aristotle University of Thessaloniki in 2018. Her research interests lie in the areas of 5G/6G wireless networks, resource management and optimization, contract theory, game theory, and reinforcement learning.

Fisayo Sangoleye received his Bachelor's degree in Electrical and Electronics Engineering from the University of Lagos, Nigeria, in 2016. He is currently pursuing a Ph.D. degree with the Department of Electrical and Computer Engineering, University of New Mexico. His main research interests include resource allocation in wireless networks, artificial intelligence, and demand response management in smart grid networks. He is a member of the National Society of Black Engineers (NSBE).

Eirini Eleni Tsiropoulou is an Assistant Professor at the Department of Electrical and Computer Engineering, University of New Mexico. Her main research interests lie in the area of cyber-physical social systems, reinforcement learning, game theory, and network economics. She was selected by the IEEE Communication Society - N2Women - as one of the top ten Rising Stars of 2017 in the communications and networking field, while she received the Early Career Award by the IEEE Communications Society Internet Technical Committee in 2019.

Symeon Papavassiliou is a Professor in the School of Electrical and Computer Engineering (ECE) at National Technical University of Athens. From 1995 to 1999, he was a senior technical staff member at AT&T Laboratories, New Jersey. In August 1999 he joined the ECE Department at the New Jersey Institute of Technology, USA, where he was an Associate Professor until 2004. He has an established record of publications, with more than 350 journal and conference published papers, in the areas of modeling and optimization of complex systems.